

Energy gap, penetration depth, and surface resistance of MgB₂ thin films determined by microwave resonator measurements

B. B. Jin* and N. Klein

Forschungszentrum Jülich, Institute of Thin Films and Interfaces, D-52425 Jülich, Germany

W. N. Kang, Hyeong-Jin Kim, Eun-Mi Choi, and Sung-Ik Lee

National Creative Research Initiative Center for Superconductivity, Department of Physics, Pohang University of Science and Technology, Pohang 790-784, Republic of Korea

T. Dahm

Universität Tübingen, Institut für Theoretische Physik, Auf der Morgenstelle 14, 72076 Tübingen, Germany

K. Maki

Department of Physics and Astronomy, University of Southern California, Los Angeles, California 90089-0484

(Received 19 April 2002; revised manuscript received 21 June 2002; published 27 September 2002)

We have measured the temperature dependence of the microwave surface impedance $Z_s = R_s + i\omega\mu_0\lambda$ of two *c*-axis oriented MgB₂ films employing dielectric resonator techniques. The temperature dependence of the magnetic-field penetration depth λ determined by a sapphire dielectric resonator at 17.9 GHz can be well fitted from 5 K close to T_c by the standard BCS integral expression assuming the reduced energy gap $\Delta(0)/kT_c$ to be as low as 1.13 and 1.03 for the two samples. For the penetration depth at zero temperatures, values of 102 and 107 nm were determined from the fit. Our results clearly indicate the *s*-wave character of the order parameter. A similar fit of the penetration depth data was obtained with an anisotropic *s*-wave BCS model. Within this model we had to assume a prolate order parameter, having a large gap value in the *c*-axis direction and a small gap within the *ab* plane. This is in contrast to recent fits of the anisotropic *s*-wave model to upper critical-field data, where an oblate order parameter had to be used, and raises interesting questions about the nature of the superconducting state in MgB₂. A rutile dielectric resonator was employed to obtain the temperature dependence of R_s with high accuracy. Below about $T_c/2$, $R_s(T) - R_s(5\text{ K})$ exhibits an exponential temperature dependence with a reduced energy gap consistent with that determined from the penetration depth data. The R_s value at 4.2 K was found to be as low as 19 $\mu\Omega$ at 7.2 GHz, which is comparable with a high-temperature superconducting copper oxide thin film.

DOI: 10.1103/PhysRevB.66.104521

PACS number(s): 74.25.Nf, 07.57.Pt, 74.70.Ad

The question about the energy gap in a particular superconducting material is of fundamental importance for the understanding of the relevant pairing mechanism and for the determination of its application potential. In the case of MgB₂ this question is raised with particular emphasis.¹ According to initial findings, MgB₂ seemed to comprise a relatively high transition temperature (around 40 K) with superconducting properties resembling those of conventional superconductors rather than those of high-temperature superconducting (HTS) cuprates.^{2–4} Recent experiments have brought some clarifications about the gap features of MgB₂. According to tunneling spectroscopy,^{5,6} point-contact spectroscopy,^{7,8} photoemission,⁹ Raman scattering,¹⁰ specific heat,^{11,12} and optical conductivity spectra,¹³ there is evidence for an *s*-wave symmetry of order parameters with two energy gaps, which are much lower and larger than the BCS weak-coupling value ($\Delta/kT_c = 1.76$). The isotropic two-gap model or the anisotropic one-gap model are proposed to explain these observations.^{14–18} On a qualitative level, they have similar properties, and therefore more experimental efforts are required to distinguish between these two theories.

On the other hand, the results for the temperature dependence of the penetration depth $\lambda(T)$ are quite controversial. Quadratic, linear, and exponential dependences were re-

ported in the literature.^{19–28} Quadratic and linear dependence might be an indication for unconventional superconductivity, similar to HTS cuprates.^{29–33} However, the observation of an exponential dependence would be a clear indication for a nodeless gap, i.e., for an order parameter comprising *s*-wave symmetry. Hence, a very high measurement accuracy for temperature changes of λ at $T \ll T_c$ for high-quality samples is required to distinguish between a power-law and an exponential temperature dependence.

Microwave surface impedance measurements have proved to be the most sensitive tool to determine the temperature dependence of λ of both thin-film^{29–31} and bulk single-crystal samples.³² In particular, they have been employed successfully to attain significant information about the symmetry of the order parameter in the high-temperature superconducting cuprates.³³ Therefore, microwave resonator techniques are most appropriate to be used for high-precision $\lambda(T)$ measurements on high-quality MgB₂ samples.

Apart from the penetration depth, the microwave surface resistance R_s is an important figure of merit for microwave applications. According to the BCS theory, the expected $\exp(-\Delta/kT)$ dependence of R_s below $T_c/2$ might result in low R_s values at temperatures attainable with low-power cryocoolers.

MgB₂ thin films were fabricated using a two-step method by pulsed laser deposition. The detailed process is described in Refs. 34 and 35. The films deposited on a plane parallel [1102]-oriented sapphire substrate of 10×10 mm² in size exhibit a sharp resistive and inductive transition at transition temperatures up to 39 K (onset temperature of resistive transition). The film thickness was 400 nm for both samples. X-ray diffraction analysis indicates a high degree of *c*-axis orientation perpendicular to the substrate surface and no detectable amount of MgO or any other crystalline impurity phases.

The microwave surface impedance was determined using a sapphire dielectric resonator technique described elsewhere.³⁶ The cavity with part of one end plate replaced by the thin-film sample was excited in the TE_{01δ} mode under weak-coupling conditions. The unloaded quality factor Q_0 and resonant frequency was recorded as a function of temperature. The real part of the effective surface impedance, the effective surface resistance R_s^{eff} , was determined according to

$$R_s^{\text{eff}}(T) = G \left[\frac{1}{Q_0(T)} - \frac{1}{Q_{\text{Nb}}(4.2 \text{ K})} \right], \quad (1)$$

with G being a geometrical factor determined by a numerical simulation of the electromagnetic field distribution in the cavity and $Q_{\text{Nb}}(4.2 \text{ K}) = 108\,440$, representing the unloaded quality factor measured by employing a high-quality Nb thin film as the sample. The notation “effective” indicates an enhancement of R_s and λ due to the film thickness d being of the order of λ .³⁷ For temperatures below 30 K, Eq. (1) allows for the determination of R_s^{eff} with a systematic error of about 0.1 mΩ, which is due to neglecting the temperature-dependent background losses of the cavity and the small microwave losses ($R_s \approx 10^{-5} \Omega$) of the Nb film.

The temperature dependence of the effective penetration depth was determined from the temperature dependence of the resonant frequency $f(T)$, using

$$\delta\lambda^{\text{eff}}(T) = - \frac{G}{\pi\mu_0} \frac{f(T) - f(5 \text{ K})}{f^2(5 \text{ K})} \quad (2)$$

with $\mu_0 = 1.256 \times 10^{-6} \text{ V s/A m}$. There is a systematic error due to frequency changes caused by thermal expansion, the temperature dependence of the skin depth of the cavity wall material (copper), and the temperature dependence of the dielectric constant of sapphire. To account for these effects, we recorded the temperature dependence of the resonant frequency employing a copper sample. From this measurement we found that the systematic error is less than 1 nm for $T \leq 15 \text{ K}$ and less than 2.5 nm for $T \leq 25 \text{ K}$, which is at least one order of magnitude lower than the observed temperature changes of λ for our MgB₂ samples. Therefore, Eq. (2) was applied without correction for our investigation.

In general, microwave resonator measurements do not allow for the determination of absolute values of λ because the resonator dimensions are only known with a precision of several ten’s of micrometers. However, absolute values of λ can be extracted by comparing the measured temperature de-

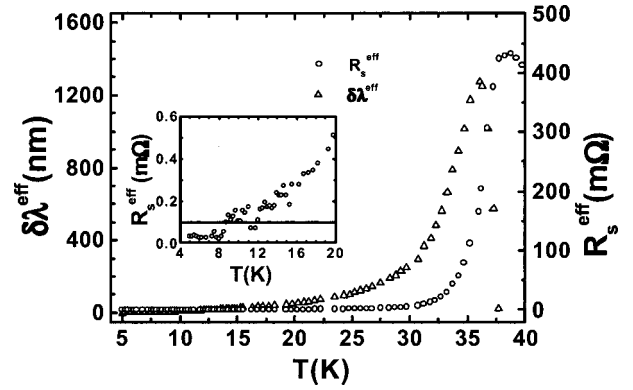


FIG. 1. Temperature dependence of R_s^{eff} and $\delta\lambda^{\text{eff}}$ of a MgB₂ thin film recorded at 17.9 GHz using a dielectric (sapphire) resonator technique. The inset shows the $R_s^{\text{eff}}(T)$ values below 8 K and our measurement resolution of 100 $\mu\Omega$.

pendence with existing models. Of course, it is worth investigating how to measure the absolute penetration depth of superconducting thin film.³⁸

Two samples (S0716 and S1030) were measured and a similar temperature dependence of Z_s was observed. Figure 1 shows one of the temperature dependences of R_s^{eff} and $\delta\lambda^{\text{eff}}$ (S1030) as determined by Eqs. (1) and (2), respectively. The inset shows the $R_s^{\text{eff}}(T)$ data at low temperatures. The full line represents the resolution limit of our setup. Below 8 K, R_s^{eff} is below the resolution of our technique (100 $\mu\Omega$).

Figure 2 shows the measured temperature dependence of $\delta\lambda^{\text{eff}}$ determined from $f(T)$ according to Eq. (2) in a $\log_{10}(\delta\lambda)$ versus $1/T$ representation. The horizontal axis is drawn in the reciprocal form of T . Experiments indicate that the coherence length ξ and penetration depth λ are about 5 and 100 nm, so that $\lambda/\xi > 1$.³⁹ This is in the reasonably local regime. In this case $\lambda(T)$ based on the standard BCS model can be represented as follows:

$$\frac{1}{\lambda^2(T)} = \frac{1}{\lambda^2(0)} \left[1 - 2 \int_{\Delta(T)}^{\infty} \frac{\partial f(\varepsilon)}{\partial \varepsilon} \frac{\varepsilon}{\sqrt{\varepsilon^2 - \Delta^2(T)}} d\varepsilon \right], \quad (3)$$

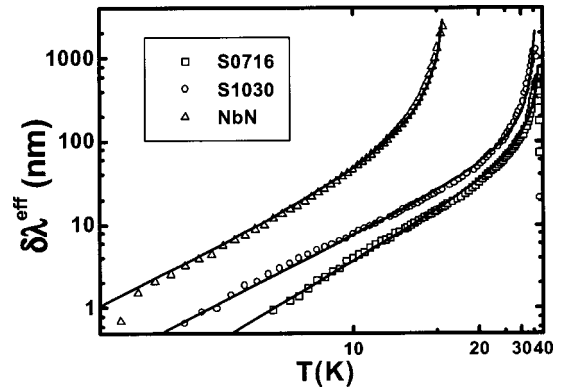


FIG. 2. $\log_{10}(\delta\lambda^{\text{eff}})$ vs $1/T$ representation of the penetration depth data for two MgB₂ samples and a NbN thin film for comparison. The solid line represents BCS fits with parameters as described in the text.

with $f(\varepsilon)=[\exp(\varepsilon/kT)+1]^{-1}$ representing the Fermi function and $\Delta(T)$ the temperature dependence of energy gap. The quantities $\Delta(0)/kT_c$ and $\lambda(0)$ are used as fit parameters. For the temperature dependence of $\Delta(T)/\Delta(0)$ values tabulated in Ref. 40 were used. The full lines represent BCS calculations. The $\delta\lambda_{\text{BCS}}$ values calculated from Eq. (3) are multiplied with $\coth(d/\lambda_{\text{BCS}})$ to account for the finite film thickness.³⁷ As a result, the fits of Eq. (3) to the $\delta\lambda_{\text{eff}}(T)$ data (full lines in Fig. 2) yield $\Delta(0)/kT_c=1.13$, $T_c=39$ K [$\Delta(0)=3.8$ meV], and $\lambda(0)=102$ nm for sample S0716; $\Delta(0)/kT_c=1.03$, $T_c=36$ K [$\Delta(0)=3.2$ meV], and $\lambda(0)=107$ nm for sample S1030. According to Fig. 2, there is a very good agreement between experimental data and the fit curves over the entire temperature range. The down-turn of the experimental data very close to T_c can be explained by impedance transformations resulting from the finite film thickness.³⁷ The nearly linear dependence below $T_c/2$ in this representation clearly indicates the s -wave nature of the order parameter, i.e., a finite-energy gap in all directions of the Fermi surface without nodes. In contrast, a double-logarithmic plot of the same data indicates that a power law does not fit the data at low temperatures. For comparison, the same analysis was performed for a NbN thin film, which is a well-known s -wave superconductor with a relatively high T_c of 15.8 K.⁴¹ The fit parameters are $\Delta(0)/kT_c=2.3$ and $\lambda(0)=225$ nm, respectively, which is similar to literature data.⁴²

The $\Delta(0)/kT_c$ values obtained for the MgB₂ samples are comparable with the value of 3.5 ± 0.5 meV determined by scanning tunneling microscopy.⁵ The $\lambda(0)$ values are also in the range of corresponding values determined by other techniques.^{19,23,43,44} In contrast to tunneling experiments, which are very sensitive to a possible modification of the surface, microwave surface impedance measurements probe almost the entire volume of a thin-film sample with thickness of the order of λ . Therefore, surface degradation can be ruled out as a possible reason for the small values of Δ/kT_c . In fact, some tunneling data exhibit Δ/kT_c values even lower than ours, indicating that surface degradation effects may play some role there.³

The low $\Delta(0)/kT_c$ (<1.76 , BCS weak-coupling limit) is difficult to understand within a standard BCS-type s -wave theory, but can be explained by an isotropic two-gap or anisotropic one-gap model.^{14–18} Then, the small gap represents the smallest component of a double or a strongly anisotropic gap. In this case, the temperature dependence of λ at $T \ll T_c$ would be determined by its minimum values, because $\lambda(T)$ probes the thermal excitations with the lowest activation energy. However, the existence of a second large gap should have a significant impact on $\lambda(T)$ at higher temperatures. Figure 3 shows the temperature dependence of $\lambda^2(0)/\lambda^2(T)$, which represents the normalized superfluid density. As expected from Fig. 2, a very good agreement with a single-gap BCS theory is achieved for both samples. Similar to the MgB₂ samples, the NbN film also exhibits a very good agreement over the entire temperature range. The latter indicates that the effects of strong coupling on $\lambda(T)$

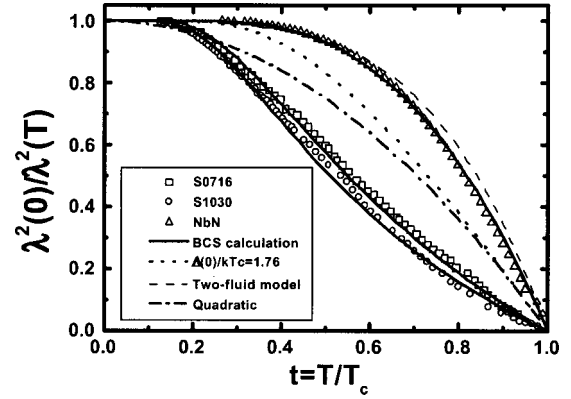


FIG. 3. $\lambda^2(0)/\lambda^2(T)$ dependence for the samples shown in Fig. 2. The full lines represent BCS fits using $\Delta(0)/kT_c$ as fit parameter. The predictions by two-fluid model (dashed), quadratic (dash-dotted) dependence, and standard BCS model with $\Delta(0)/kT_c=1.76$ (dotted) are also drawn.

can still be modeled by the BCS integral expression just by assuming Δ/kT_c to be larger than the BCS value of 1.76.⁴⁵

For comparison, the power-law dependence $[\lambda(0)/\lambda(T)]^2=1-(T/T_c)^n$ with $n=2$ (“quadratic”) and $n=4$ (“two-fluid model”) is also depicted in Fig. 3. Above about $T_c/2$, $n=4$ represents a fairly good approximation for the case of strong coupling, as observed for NbN. However, there is a clear discrepancy between the experimental data and quadratic dependence, ruling out the possibility of unconventional superconductivity in MgB₂.

Obviously, our data do not show any indication of a second larger energy gap. Before discussing the reason, it should be noted that the penetration depth studied here is in fact the penetration depth in the ab plane (λ_{ab}) due to the samples being c -axis oriented thin films. In the two-gap or multigap scenarios, the superconductivity mainly comes from the boron (B) orbital in the ab plane. The E_{2g} phonons, which involve in-plane displacements, couple strongly to the B p_{xy} electronic bands and yield strong electron-phonon interactions.^{14,15} Two isotropic energy gaps are predicted in the clean limit.¹⁶ One is associated with a two-dimensional (2D) bonding σ band having a larger energy gap than the BCS value, i.e., $\Delta(0)/kT_c > 1.76$. The other is associated with 3D bonding and antibonding π bands having a smaller energy gap less than the BCS value, i.e., $\Delta(0)/kT_c < 1.76$. The two bands have some coupling to give a single T_c . Hence, the small $\Delta(0)/kT_c$ observed in our measurement would correspond to the small energy gap in the two-gap model, and the superfluid density should be affected by the large energy gap in the high-temperature region. Another alternative explanation suggests an anisotropic s -wave order parameter due to its anisotropic crystal structure.¹⁷ An ellipsoidal energy-gap function is assumed with a minor axis within the ab plane and a major axis along the c direction. This model predicts that λ_{ab} is mainly determined by the small energy gap, which is consistent with our measurement.

In Fig. 4 we show the calculations of the ab -plane superfluid density (solid lines) within the anisotropic one-gap

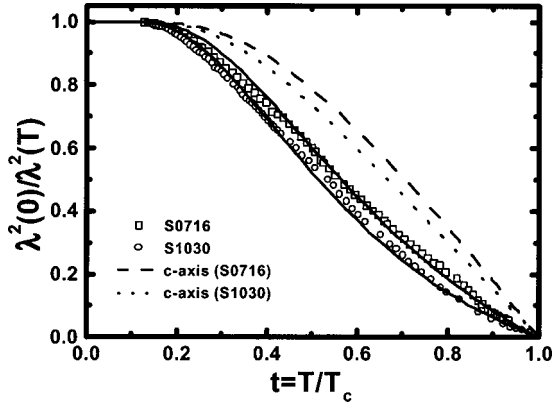


FIG. 4. Fitting of the $\lambda^2(0)/\lambda^2(T)$ dependence to experimental results (symbols) with an anisotropic s -wave one-gap model (solid lines). The fitting parameters of the maximum gap $\Delta_{\max}(0)/kT_c$ and minimum gap $\Delta_{\min}(0)/kT_c$ are 3.85 and 1.09 for sample S0716, and 4.49 and 0.97 for sample S1030, respectively. The dashed lines (for sample S0716) and dotted lines (for sample S1030) show the corresponding c -axis penetration depth temperature dependences expected from this model.

model and compare them with the measurements (symbols) above. Here, an elliptical angular dependence of the gap having the form

$$\Delta(\vartheta) = \frac{\Delta_{\min}}{\sqrt{1 - a \cos^2 \vartheta}} \quad (4)$$

has been used. The angle ϑ is the polar angle with respect to the c axis, $\vartheta=0$ corresponding to the c -axis direction and $\vartheta=\pi/2$ corresponding to the ab -plane direction. The parameter a ($0 < a < 1$) determines the anisotropy ratio $\gamma = \Delta_{\max}/\Delta_{\min} = 1/\sqrt{1-a}$. We emphasize that this parameter is our only fitting parameter. The temperature dependence of the gap and the gap ratios $\Delta_{\max}(T=0)/kT_c$ and $\Delta_{\min}(T=0)/kT_c$ are determined from a self-consistent solution of the anisotropic weak-coupling gap equation. (For more details, see Refs. 17 and 18). The best fit to sample S0716 is obtained for $\gamma=3.53$, yielding a maximum gap $\Delta_{\max}(T=0)/kT_c=3.85$ and a minimum gap $\Delta_{\min}(T=0)/kT_c=1.09$. For sample S1030, we find $\gamma=4.61$ with $\Delta_{\max}(0)/kT_c=4.49$ and $\Delta_{\min}(0)/kT_c=0.97$. These anisotropy ratios are somewhat bigger than single-crystal measurements $\gamma=2.5$,⁷ but are roughly in line with an analysis of specific-heat data.⁴⁶ Therefore, we can conclude that our results are consistent with an anisotropic one-gap model, possessing a small gap in the ab -plane direction.

Within this anisotropic s -wave model we can also calculate the c -axis superfluid density. For comparison, this quantity is shown in Fig. 4 for the same parameters (dashed line for sample S0716 and dotted line for sample S1030). We cannot measure the c -axis penetration depth with our current experimental setup. Such a measurement would give a valuable comparison with the prediction of the anisotropic one-gap model and is left for a future study.

The anisotropy of the penetration depth is related to the anisotropy of the lower critical field H_{c1} via the relation

$H_{c1}^c/H_{c1}^{ab} = \lambda_c/\lambda_{ab}$.⁴⁷ In experimental studies of H_{c1} on MgB_2 it has been observed that H_{c1} is somewhat bigger in the ab -plane direction than in the c -axis direction.^{48,49} This is consistent with our findings here.⁵⁰ However, the upper critical field H_{c2} is also bigger in the ab -plane direction than in the c -axis direction.^{48,49,51} This appears to be inconsistent with the H_{c1} anisotropy within the anisotropic Ginzburg-Landau theory from which one should have expected $H_{c1}^c/H_{c1}^{ab} = H_{c2}^{ab}/H_{c2}^c$.⁴⁷ In Ref. 18 it has been shown that this H_{c2} anisotropy can be understood within the anisotropic s -wave model, if the maximum gap is assumed to lie within the ab plane and the small gap in the c -axis direction (oblate form of the gap anisotropy), in contrast to what we need to fit our data here. Thus, it appears that high-magnetic-field data are governed by a different anisotropy of the gap than low-field data. This puzzling discrepancy is reinforced by our experimental findings and can be neither understood within the isotropic two-band nor within the anisotropic one-gap model in the present form. A possible solution to this problem could be a strong field dependence of the anisotropy of the gap or possibly a fully anisotropic two-gap model.⁵¹ But this remains speculation at this point and more experimental as well as theoretical investigations are necessary to clarify this problem.

We want to mention here that our data have been fitted also within the two-gap model recently by Golubov *et al.*⁵² In these fits a very small value of the penetration depth of 39.2 nm had to be assumed, which is much smaller than the values of the order of 100 nm we determined here. Golubov *et al.* also showed that within their two-gap model, the c -axis superfluid density is expected to be smaller than the ab -plane superfluid density, in contrast to the prediction of our prolate model here. Besides this being inconsistent with the aforementioned H_{c1} data, this difference in the c -axis response could be used for an experimental test between these two models. Thus, a measurement of the temperature dependence of the c -axis penetration depth would be highly desirable.

As mentioned above, the measurement accuracy of R_s at low temperature is limited by the resolution of our setup. Sapphire has a low dielectric constant (~ 10) and leads to a large leakage field outside the dielectric resonator. This field induces currents on the walls of the copper cavity, leading to a strong limitation of the Q value due to the loss contribution of copper. In order to achieve a higher resolution, the sapphire puck was replaced by a rutile dielectric puck of similar dimensions.⁵³ Rutile has a high dielectric constant (~ 100 in ab plane) resulting in a lower frequency of 7.18 GHz for the $\text{TE}_{01\delta}$ mode. Due to the high dielectric constant of rutile, the electromagnetic field is well confined inside the puck. Consequently, the ratio of losses in the superconducting film and in the copper shield is increased by a factor of 10. From Eq. (1) we know that a distinguishable difference of Q values for Nb and MgB_2 thin films is the key to get accurate R_s . In our measurement, Q values at 4.2 K for Nb and sample S1030 are 1.29×10^6 and 1.20×10^6 , respectively, which yields an R_s of $19.4 \mu\Omega$. Frequency scaling according to an assumed square law results in $R_s = 37.6 \mu\Omega$ at 10 GHz, which is comparable to high-quality yttrium-barium-copper-oxide (YBCO) thin film. This value is also in accordance with data

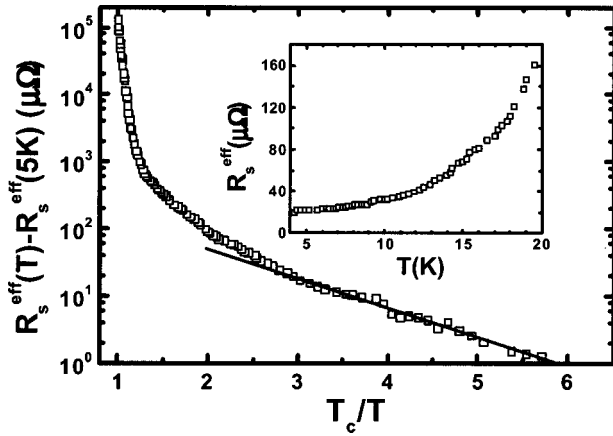


FIG. 5. $R_s^{\text{eff}}(T) - R_s^{\text{eff}}(T=5\text{ K})$ measured at 7.18 GHz plotted versus T_c/T representation for the sample S1030. The temperature dependence of R_s^{eff} below 20 K is shown in the inset. The full lines correspond to an exponential fit with $\Delta(0)/kT_c$ obtained from the sapphire resonator measurement.

obtained by another group.⁵⁴ However, it should be noted that the rutile resonator is not suitable for penetration depth measurement due to a large temperature coefficient of the dielectric constant of rutile. Figure 5 shows the temperature dependence of $R_s^{\text{eff}} - R_s^{\text{eff}}(5\text{ K})$ for sample S1030. The linear behavior at low temperature implies an s -wave symmetry of the order parameter. The full line corresponds to an $\exp(-\Delta/kT)$ behavior with a Δ/kT_c value as determined from the penetration depth data. The inset of Fig. 5 shows the temperature dependence of R_s^{eff} below 20 K. In addition, the normal-state resistivity ρ can also be derived from R_s^{eff} . As T approaches T_c , the penetration depth goes to infinity. So, the skin depth from normal-state electrons dominates the

high-frequency shielding. Using $R_s^{\text{eff}} = 127\text{ m}\Omega$ from Fig. 5 at T very close to T_c we obtained $\rho \approx R_s^{\text{eff}} d = 5\text{ }\mu\Omega\text{ cm}$, which is similar with dc measurements.³⁴ From this we can get a rough estimate of the mean free path in our films. Taking a Fermi velocity of $v_F = 4.8 \times 10^7\text{ cm/s}$,¹⁴ a carrier density of $n = 6.7 \times 10^{22}/\text{cm}^3$, and the free-electron mass, we find $l \approx 5\text{ nm}$, which is about as big as the coherence length.⁴³ We conclude that our films are neither in the dirty limit nor in the fully clean limit, but in the intermediate clean limit.

In conclusion, our experimental finding represents clear evidence for the existence of a finite gap with $\Delta(0)/kT_c$ values around 1.1. The temperature dependence of λ can be well fitted by the BCS theory in the entire temperature range below T_c , together with $\lambda(0)$ of about 100 nm. This measurement is consistent with an anisotropic one-gap model, together with an ellipsoidal energy gap function having a minimum within the ab plane and a maximum along the c axis. Our data can also be fitted within a two-gap model; however a much smaller penetration depth has to be assumed. In order to distinguish between these two theoretical models, measurements of the c -axis penetration depth or the c -axis microwave response would be desirable. We also pointed out a puzzling discrepancy between the gap anisotropy as extracted from high-magnetic-field data on one hand and low-magnetic-field data, as our penetration depth data, on the other hand. The low R_s value ($19.4\text{ }\mu\Omega$ at 4.2 K, $170\text{ }\mu\Omega$ at 20 K and 7.18 GHz) obtained for one sample implies that MgB_2 is a promising material for microwave applications.

We thank Dr. Z. Wang, KARC Communications Research Lab, Japan, for providing NbN thin films. The work at Postech was supported by the Ministry of Science and Technology of Korea through the Creative Research Initiative Program.

*Corresponding author. Email address: b.b.jin@fz-juelich.de

¹J. Nagamatsu, N. Nakagawa, T. Muranaka, Y. Zenitani, and J. Akimitsu, *Nature (London)* **410**, 63 (2001).

²S. L. Bud'ko, G. Lapertot, C. Petrovic, C. E. Cunningham, N. Anderson, and P. C. Canfield, *Phys. Rev. Lett.* **86**, 1877 (2001).

³G. Karapetrov, M. Iavarone, W. K. Kwok, G. W. Crabtree, and D. G. Hinks, *Phys. Rev. Lett.* **86**, 4374 (2001).

⁴H. Schmidt, J. F. Zasadzinski, K. E. Gray, and D. G. Link, *Phys. Rev. B* **63**, 220504(R) (2001).

⁵F. Giubileo, D. Roditchev, W. Sacks, R. Lamy, D. X. Thanh, J. Klein, S. Miraglia, D. Fruchart, J. Marcus, and Ph. Monod, *Phys. Rev. Lett.* **87**, 177008 (2001).

⁶P. Seneor, C. T. Chen, N. C. Yeh, R. P. Vasquez, L. D. Bell, C. U. Jung, Min-Seok Park, Heon-Jung Kim, W. N. Kang, and Sung-Ik Lee, *Phys. Rev. B* **65**, 012505 (2002).

⁷P. Szabo, P. Samuely, J. Kacmarcik, T. Klein, J. Marcus, D. Fruchart, S. Miraglia, C. Marcena, and A. G. M. Jansen, *Phys. Rev. Lett.* **87**, 137005 (2001).

⁸H. Schmidt, J. F. Zasadzinski, K. E. Gray, and D. G. Hinks, *Phys. Rev. Lett.* **88**, 127002 (2002).

⁹S. Tsuda, T. Yokoya, T. Kiss, Y. Takano, K. Togano, H. Kito, H. Ihara, and S. Shin, *Phys. Rev. Lett.* **87**, 177006 (2001).

¹⁰X. K. Chen, M. J. Konstantinovic, J. C. Irwin, D. D. Lawrie, and

J. P. Franck, *Phys. Rev. Lett.* **87**, 157002 (2001).

¹¹F. Bouquet, R. A. Fisher, N. E. Phillips, D. G. Hinks, and J. D. Jorgensen, *Phys. Rev. Lett.* **87**, 047001 (2001).

¹²H. D. Yang, J. Y. Lin, H. H. Li, F. H. Hsu, C. J. Liu, S. C. Li, R. C. Yu, and C. Q. Jin, *Phys. Rev. Lett.* **87**, 167003 (2001).

¹³J. J. Tu, G. L. Carr, V. Perebeinos, C. C. Homes, M. Strongin, P. B. Allen, W. N. Kang, Eun-Mi Choi, Hyeong-Jin Kim, and Sung-Ik Lee, *Phys. Rev. Lett.* **87**, 277001 (2001).

¹⁴J. Kortus, I. I. Mazin, K. D. Belashchenko, V. P. Antropov, and L. L. Boyer, *Phys. Rev. Lett.* **86**, 4656 (2001).

¹⁵J. M. An and W. E. Pickett, *Phys. Rev. Lett.* **86**, 4366 (2001).

¹⁶A. Y. Liu, I. I. Mazin, and J. Kortus, *Phys. Rev. Lett.* **87**, 087005 (2001).

¹⁷S. Haas and K. Maki, *Phys. Rev. B* **65**, 020502(R) (2002).

¹⁸A. I. Posazhennikova, T. Dahm, and K. Maki, *cond-mat/0204272*, *Europhys. Lett.* (to be published).

¹⁹C. Panagopoulos, B. D. Rainford, T. Xiang, C. A. Scott, M. Kambara, and I. H. Inoue, *Phys. Rev. B* **64**, 094514 (2001).

²⁰A. V. Pronin, A. Pimenov, A. Loidl, and S. I. Krasnosvobodtsev, *Phys. Rev. Lett.* **87**, 097003 (2001).

²¹R. A. Kaindl, M. A. Carnahan, J. Orenstein, D. S. Chemla, H. M. Christen, H. Y. Zhai, M. Paranthaman, and D. H. Lowndes, *Phys. Rev. Lett.* **88**, 027003 (2002).

- ²²S. L. Li, H. H. Wen, Z. W. Zhao, Y. M. Ni, Z. A. Ren, G. C. Che, H. P. Yang, Z. Y. Liu, and Z. X. Zhao, *Phys. Rev. B* **64**, 094522 (2001).
- ²³A. A. Zhukov, L. F. Cohen, A. Purnell, Y. Bugoslavsky, A. Berenov, J. L. MacManus-Driscoll, H. Y. Zhai, H. M. Christen, M. P. Paranthaman, D. H. Lowndes, M. A. Jo, M. C. Blamir, L. Hao, and J. Gallop, cond-mat/0107240 (unpublished).
- ²⁴N. Klein, B. B. Jin, J. Schubert, M. Schuster, H. R. Yi, A. Pimenov, A. Loidl, and S. I. Krasnoosvobodtsev, cond-mat/0107259 (unpublished).
- ²⁵G. Lamura, E. Di Gennaro, M. Salluzzo, A. Andreone, J. Le Cochec, A. Gauzzi, C. Cantoni, M. Paranthaman, D. K. Christen, H. M. Christen, G. Giunchi, and S. Ceresara, *Phys. Rev. B* **65**, 020506(R) (2002).
- ²⁶R. Prozorov, R. W. Giannetta, S. L. Bud'ko, and P. C. Canfield, *Phys. Rev. B* **64**, 180501(R) (2002).
- ²⁷F. Manzano, A. Carrington, N. E. Hussey, S. Lee, A. Yamamoto, and S. Tajima, *Phys. Rev. Lett.* **88**, 047002 (2002).
- ²⁸M.-S. Kim, J. A. Skinta, T. R. Lemberge, W. N. Kang, H.-J. Kim, E.-M. Choi, and S.-I. Lee, *Phys. Rev. B* **66**, 064511 (2002).
- ²⁹N. Klein, Jülich Research Center Internal Report No. Jül-3773, 1997 (unpublished).
- ³⁰M. R. Trunin, *Phys. Usp.* **41**, 843 (1998).
- ³¹S. Hensen, G. Müller, C. T. Rieck, and K. Scharnberg, *Phys. Rev. B* **56**, 6237 (1997).
- ³²W. N. Hardy, D. A. Bonn, D. C. Morgan, Ruixing Liang, and Kuan Zhag, *Phys. Rev. Lett.* **70**, 3999 (1993).
- ³³M. A. Hein, *High-Temperature Superconductor Thin Films at Microwave Frequency*, Springer Tracts of Modern Physics Vol. 155 (Springer, Heidelberg, 1999).
- ³⁴W. N. Kang, H.-J. Kim, E.-M. Choi, C. U. Jung, and Sung-Ik Lee, *Science* **292**, 1521 (2001).
- ³⁵H.-J. Kim, W. N. Kang, E.-M. Choi, M.-S. Kim, Kijoon H. P. Kim, and S.-I. Lee, *Phys. Rev. Lett.* **87**, 087002 (2001).
- ³⁶N. Klein, U. Dähne, U. Poppe, N. Tellmann, K. Urban, S. Orbach, S. Hensen, G. Müller, and H. Piel, *J. Supercond.* **5**, 195 (1992); N. Klein, German Patent No. DE 42 04 369 C2 (25 August 1994); U.S. Patent No. 5,506,497 (9 April 1996).
- ³⁷N. Klein, H. Chaloupka, G. Müller, S. Orbach, H. Piel, B. Rosa, L. Schultz, U. Klein, and M. Peiniger, *J. Appl. Phys.* **67**, 6940 (1990).
- ³⁸R. Prozorov, R. W. Giannetta, A. Carrington, P. Fournier, R. L. Greene, P. Guptasarma, D. G. Hinks, and A. R. Banks, *Appl. Phys. Lett.* **77**, 4202 (2000).
- ³⁹P. C. Canfield, D. K. Finnemore, S. L. Bud'ko, J. E. Ostenson, G. Lapertot, C. E. Cunningham, and C. Petrovic, *Phys. Rev. Lett.* **86**, 2423 (2001).
- ⁴⁰B. Mühlischlegel, *Z. Phys.* **155**, 313 (1959).
- ⁴¹Z. Wang, A. Kawakami, Y. Uzawa, and B. Komiyama, *Appl. Phys. Lett.* **64**, 2034 (1994).
- ⁴²B. Komiyama, Z. Wang, and M. Tonouchi, *Appl. Phys. Lett.* **68**, 562 (1996).
- ⁴³D. K. Finnemore, J. E. Ostenson, S. L. Bud'ko, G. Lapertot, and P. C. Canfield, *Phys. Rev. Lett.* **86**, 2420 (2001).
- ⁴⁴X. H. Chen, Y. Y. Xue, R. L. Meng, and C. W. Chu, *Phys. Rev. B* **64**, 172501 (2001).
- ⁴⁵J. P. Turneaure, J. Halbritter, and H. A. Schwetman, *J. Supercond.* **4**, 341 (1991).
- ⁴⁶F. Bouquet, Y. Wang, R. A. Fisher, D. G. Hinks, J. D. Jorgensen, A. Junod, and N. E. Phillips, *Europhys. Lett.* **56**, 856 (2001).
- ⁴⁷M. Tinkham, *Introduction to Superconductivity*, 2nd ed. (McGraw-Hill, New York, 1996), Eq. (9.8).
- ⁴⁸M. Xu, H. Kitazawa, Y. Takano, J. Ye, K. Nishida, H. Abe, A. Matsushita, N. Tsujii, and G. Kido, *Appl. Phys. Lett.* **79**, 2779 (2001).
- ⁴⁹C. Buzea and T. Yamashita, *Supercond. Sci. Technol.* **14**, R115 (2001).
- ⁵⁰T. Dahm, A. I. Posazhennikova, and K. Maki, cond-mat/0207521, *Acta Phys. Pol. B* (to be published).
- ⁵¹M. Angst, R. Puzniak, A. Wisniewski, J. Jun, S. M. Kazakov, J. Karpinski, J. Roos, and H. Keller, *Phys. Rev. Lett.* **88**, 167004 (2002).
- ⁵²A. A. Golubov, A. Brinkman, O. V. Dolgov, J. Kortus, and O. Jepsen, *Phys. Rev. B* **66**, 054524 (2002).
- ⁵³N. Klein, C. Zuccaro, U. Dähne, H. Schulz, N. Tellmann, R. Kutzner, A. G. Zaitsev, and R. Wördenweber, *J. Appl. Phys.* **78**, 6683 (1995).
- ⁵⁴M. A. Hein, M. Getta, S. Kreiskott, B. Mönter, H. Piel, D. E. Oates, P. J. Hirst, R. G. Humphreys, H. N. Lee, and S. H. Moon, *Physica C* **372-376**, 571 (2002).